2017

Spin texture on top of flux avalanches in Nb/Al2O3/Co thin film heterostructures

R F. Lopes
Universidade Federal Do Rio Grande Do Sul, rovan.lopes@ufrgs.br

D Carmo
Federal University of Sao Carlos

F Colauto
Federal University of Sao Carlos

Wilson Aires Ortiz
Federal University of Sao Carlos

A M H De Andrade
Universidade Federal Do Rio Grande Do Sul

See next page for additional authors

Publication Details

Lopes, R. F., Carmo, D., Colauto, F., Ortiz, W. A., de Andrade, A. M. H., Johansen, T. H., Baggio-Saitovitch, E. & Pureur, P. (2017). Spin texture on top of flux avalanches in Nb/Al2O3/Co thin film heterostructures. Journal of Applied Physics, 121 (1), 013905-1 - 013905-6.

Spin texture on top of flux avalanches in Nb/Al2O3/Co thin film heterostructures

Abstract
We report on magneto-optical imaging, magnetization, Hall effect, and magneto-resistance experiments in Nb/Al2O3/Co thin film heterostructures. The magneto-transport measurements were performed in samples where electrical contacts were placed on the Co layer. The magnetic field is applied perpendicularly to the plane of the film and gives rise to abrupt flux penetration of dendritic form. A magnetization texture is imprinted in the Co layer in perfect coincidence with these ramifications. The spin domains that mimic the vortex dendrites are stable upon the field removal. Moreover, the imprinted spin structure remains visible up to room temperature. In the region of the field-temperature diagram where flux instabilities are known to occur in bare Nb films, irregular jumps are observed in the magnetic hysteresis and large amplitude noise is detected in the magneto-resistance and Hall resistivity data when measured as a function of the field.

Disciplines
Engineering | Physical Sciences and Mathematics

Publication Details
Lopes, R. F., Carmo, D., Colauto, F., Ortiz, W. A., de Andrade, A. M. H., Johansen, T. H., Baggio-Saitovitch, E. & Pureur, P. (2017). Spin texture on top of flux avalanches in Nb/Al2O3/Co thin film heterostructures. Journal of Applied Physics, 121 (1), 013905-1 - 013905-6.

Authors
R F. Lopes, D Carmo, F Colauto, Wilson Aires Ortiz, A M H De Andrade, Tom H. Johansen, E Baggio-Saitovitch, and P Pureur

Spin texture on top of flux avalanches in Nb/Al_2O_3/Co thin film heterostructures

R. F. Lopes,[1,a)] D. Carmo,[2] F. Colauto,[2,3] W. A. Ortiz,[2] A. M. H. de Andrade,[1] T. H. Johansen,[4] E. Baggio-Saitovitch,[5] and P. Pureur[1,b)]
[1]*Instituto de Física, Universidade Federal do Rio Grande do Sul, P.O. Box 15051, 91501-970 Porto Alegre, RS, Brazil*
[2]*Departamento de Física, Universidade Federal de São Carlos, 13565-905 São Carlos, SP, Brazil*
[3]*Materials Science Division, Argonne National Laboratory, Argonne, Illinois 60439, USA*
[4]*Department of Physics, University of Oslo, P. O. Box 1048 Blindern, 0316 Oslo, Norway and Institute for Superconducting and Electronic Materials, University of Wollongong, Northfields Avenue, Wollongong, NSW 2522, Australia*
[5]*Centro Brasileiro de Pesquisas Físicas, Rua Dr. Xavier Sigaud 150, 22290-180 Rio de Janeiro, RJ, Brazil*

(Received 3 August 2016; accepted 20 December 2016; published online 6 January 2017)

We report on magneto-optical imaging, magnetization, Hall effect, and magneto-resistance experiments in Nb/Al_2O_3/Co thin film heterostructures. The magneto-transport measurements were performed in samples where electrical contacts were placed on the Co layer. The magnetic field is applied perpendicularly to the plane of the film and gives rise to abrupt flux penetration of dendritic form. A magnetization texture is imprinted in the Co layer in perfect coincidence with these ramifications. The spin domains that mimic the vortex dendrites are stable upon the field removal. Moreover, the imprinted spin structure remains visible up to room temperature. In the region of the field-temperature diagram where flux instabilities are known to occur in bare Nb films, irregular jumps are observed in the magnetic hysteresis and large amplitude noise is detected in the magneto-resistance and Hall resistivity data when measured as a function of the field. *Published by AIP Publishing.* [http://dx.doi.org/10.1063/1.4973529]

I. INTRODUCTION

The study of non-collinear spin configurations structured at meso and microscopic scales has been a subject of great interest for fundamental and applied research. Initially, these investigations were devoted to the understanding of the microscopic mechanisms leading to non-trivial spin arrangements.[1] Currently, many of these structures may have potential application in innovative processes involving data manipulation or spintronics devices.[2]

Domain walls,[1] small magnetic domains in single or multilayered thin films with perpendicular anisotropy,[3] spontaneous bubble domains formed on the surface of a bulk ferromagnetic material with planar anisotropy,[4] and stripe domains in multilayered magnetic films[5] are just a few examples of spin textures structured at the sub-micron scale. These structures in general result from the interplay between the exchange energy, magnetocrystalline anisotropy, and dipolar interaction.

Recently, novel spin textures have been put forward. Examples are vortex- and chiral-type magnetic arrangements. Spin configurations in the form of vortices structured at the nanometric scale are usually associated with very small samples with circular geometries.[6] Chiral magnetic structures are extremely interesting since their stabilization is crucially dependent on the spin-orbit interaction.[7] Chiral spin textures, for instance, have been proposed to explain the anomalous Hall effect in the Kondo lattice $Pr_2Ir_2O_7$[8] and were observed in the surface states of the topological insulator $Bi_{1-x}Sb_x$ with ARPES experiments.[9]

A remarkable nanoscale chiral spin structure is the magnetic skyrmion, discovered a few years ago.[10,11] A skyrmion lattice was first observed in the magnetic crystal MnSi that lacks the inversion symmetry using neutron scattering.[10] Other observations of skyrmions using different experimental techniques have been reported in bulk materials and thin films.[12,13] Skyrmions are described as quasiparticles in an otherwise homogeneous magnetic medium that are formed by a local spin pointing opposite to the global magnetization that is surrounded by a whirling twist of spins.[14] These spin arrangements are stabilized by the Dzyaloshinskii-Moriya interaction, whose magnitude depends on the spin-orbit coupling.[14]

The heterostructures formed by bilayers or multilayers including ferromagnetic and superconducting thin films are potentially interesting systems to produce non-trivial magnetization textures. In principle, such hybrids can be applied to storing information by transcribing to the magnetic layer the flux offshoot from the vortices[15] or to controlling the vortex dynamics by regulating the in-plane magnetization of a magnetic stripe array.[16]

Usually the works on these hybrids have been dedicated to the study of the effects induced by the magnetic layers on the superconducting films.[17] A relatively smaller number of investigations, however, are focused in the effects of superconductivity on the spin configuration of the magnetic layers.[18–20] One interesting possibility along this line of investigation is the generation of unconventional spin

[a)]E-mail: rovan.lopes@ufrgs.br
[b)]E-mail: ppureur@if.ufrgs.br

textures in the ferromagnetic layers using the properties of the superconducting films. It seems reasonable to suppose that the Abrikosov vortex lattice of type-II superconducting layers may induce nanoscopic and non-trivial spin structures in nearby ferromagnetic layers grown from materials with strong spin-orbit coupling. Owing to the hexagonal symmetry that characterizes both the Abrikosov vortex lattice[21] and the skyrmion lattice,[10] one might expect that some chiral-type spin configuration forms on top of superconducting vortices, at least in the field limit where the distance between vortices is larger than the typical spin quasiparticle diameter.

In this article, we report on the spin texture generated in the ferromagnetic layer of a $Nb/Al_2O_3/Co$ thin film hybrid by the magnetic flux modulations in the Nb superconducting layer. The magnetic field applied perpendicularly to the superconducting film gives rise to abrupt flux penetration in the form of dendrites. A magnetization texture is imprinted in the Co layer in perfect coincidence with these ramifications. Magneto-optical imaging (MOI) experiments were carried out to observe both the flux avalanches and the imprinted spin texture. It is remarkable that the spin domains that mimic the flux dendrites remain stable when the field is removed. Moreover, the imprinted spin structure remains visible up to room temperature. Complementary magnetization, magneto-resistance (MR), and Hall effect experiments were performed in a similar sample where electrical contacts were placed on the Co film. In the region of the H-T diagram where flux instabilities are known to occur in the Nb film,[22] irregular jumps are observed in the magnetic hysteresis. The magneto-resistance and the Hall resistivity show a noisy behavior when measured in fixed temperatures under slowly varying magnetic fields. The noise in the magneto-transport measurements ceases at a characteristic field, which depends on the temperature. Using the magneto-resistance and Hall resistivity data, we were able to define the boundary of the instability region for the flux penetration.

In spite of having observed robust magnetic texture induced by flux avalanches in the ferromagnetic layer of a $Nb/Al_2O_3/Co$ hybrid, the MOI and transport experiments carried out until now do not allow us to extract information on the details of the generated spin configurations at the nanoscopic scale.

II. MATERIALS AND METHODS

Several samples of the thin film heterostructure $Nb/Al_2O_3/Co$ were made by UHV magnetron sputtering using the system Orion 8 manufactured by AJA International Inc. The base pressure of the chamber was better than 5×10^{-8} Torr and the Ar working pressure was 2 mTorr. The layer thicknesses for all the samples are 200 nm, 22 nm, and 24 nm for Nb, Al_2O_3, and Co, respectively. These thicknesses were determined by x-ray reflectometry for each film individually. The surface aspect of the metallic films is homogeneous when observed through optical microscopy. The composition of the prepared heterostructures is shown schematically in Fig. 1. First, a Nb film with $7 \times 7\,mm^2$ area was deposited on a thermally oxidized Si (100), keeping the substrate at 500 °C. Then, an Al_2O_3 layer was deposited on the Nb film covering its entire surface. Above the insulating coating, a rectangular shaped Co film with an areal size of $2 \times 4\,mm^2$ was deposited. The Al_2O_3 layer works as a spacer to prevent direct electrical contact between the superconductor and the ferromagnetic lamellae. The insulating layer also avoids the proximity effect between the metallic films. The Co film was overlaid with a thin Al_2O_3 layer to inhibit sample degradation. As a bridge to electrical contacts, six thin and small Ag pads, shown in Fig. 1, were deposited on the Al_2O_3 layer prior to the Co film growth. In the extremities of these pads, gold wires were glued with silver paint providing electrical contacts to the Co film in a way that magneto-resistance and Hall effect experiments could be carried out in this particular layer. The Ag contact pads and the rectangular Co were shaped by placing a hollowed mask on the samples before starting the deposition of these materials. In some heterostructures, additional electrical contacts were placed in order to test the superconducting layer separately. The Nb films of our samples have a critical temperature $T_c = 8.9\,K$.

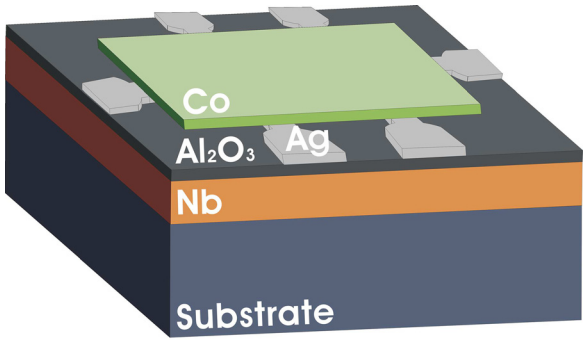

FIG. 1. Studied $Nb/Al_2O_3/Co$ heterostructure (schematic). The Si_{100} substrate has 400 μm thickness. The material layers and thicknesses are in the following sequence: Nb, 200 nm; Al_2O_3, 22 nm; Ag, 20 nm; Co, 24 nm; and not shown Al_2O_3, 10 nm.

The magnetization measurements were performed in a Quantum Design MPMS-5S@. The images were recorded in a magneto-optical imaging (MOI) setup, using a Faraday rotating Bi-substituted ferrite-garnet film with in-plane magnetization as a sensor.[23–26] Mounting the sensor plate directly on the film surface, the flux density distribution over the film area was detected as an image in a polarized light microscope with crossed polarizers. Electrical resistivity, magneto-resistance, and Hall effect measurements were carried out in a Quantum Design DynaCool Physical Properties Measuring System (PPMS). All the measurements were carried out with the magnetic field aligned perpendicularly to the sample plane.

III. RESULTS AND DISCUSSION

A. Magnetization and magneto-optical measurements

It is well known that Nb films exhibit flux avalanches when submitted to magnetic fields within a certain range and for temperatures below to approximately $T = 5\,K$.[22] We have confirmed this feature in our sample, as can be observed in Fig. 2 that shows hysteresis cycles in fields up to $\mu_0 H = \pm 20\,mT$ at four different temperatures. Before each

isothermal cycle, the sample was warmed up above T_c. At this stage, the Co layer was demagnetized by successively applying fields with alternating orientations and decreasing amplitude. The isotherms at $T = 6$ K and $T = 8$ K are smooth, as expected for a superconductor in the critical state. Consistently, the area of the hysteresis loop at $T = 6$ K is larger than that registered at $T = 8$ K. On the other hand, the isotherms at $T = 2$ K and $T = 4$ K differ from the ordinary behavior, having an areal size smaller than that in $T = 6$ K. In addition, they look strongly noisy, both in the upward and downward branches, which is well-known as a signature of flux entry in the form of avalanches.[20,24]

The avalanches develop inside the sample forming a dendritic morphology, as observed through the magneto-optical images in Figs. 3(a) and 3(b). Since the sample is larger than the microscope field of view, the magneto-optical images were taken in a fraction of the sample, which encompasses the edge between the bare Nb and the $Nb/Al_2O_3/Co$ heterostructure. Vertical lines were added to the figure in order to identify the boundary separating the uncovered Nb layer and the heterostructure. The images (a) and (b) were recorded after zero field cooling (ZFC) the sample from a temperature above T_c down to $T = 2.5$ K and the image (c) shows the remnant magnetization of the Co film after warming back the sample above T_c. In the image of Fig. 3(a), taken at $\mu_0 H = 2.5$ mT, one sees two dendritic structures that start at the edge of the sample and reach the area where the magnetic layer is located. No significant deflection or suppression of the branches is observed as the avalanches invade that area. This behavior is expected when dendrites cross the border of the covered area forming angles near $\pi/2$.[27] On the other hand, branches that are about to end at the boundary are halted. Increasing the field to $\mu_0 H = 6.0$ mT, as shown in image (b), several dendrites penetrate inside the heterostructure. When the magnetic field is removed and the sample is warmed to a temperature above T_c, the Co layer stays magnetized as shown in the image (c). Through a meticulous comparison between the images (b) and (c), one sees that several branches developed at 2.5 K are imprinted in the magnetic layer even when the Nb film is out of the superconducting state.

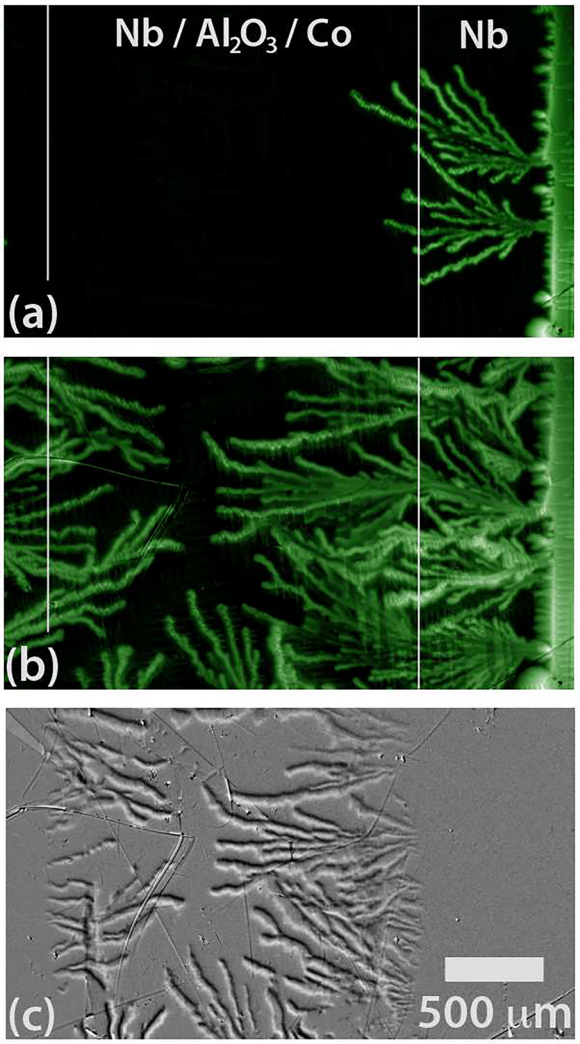

FIG. 3. Magneto-optical imaging (a) 2.5 K and 2.5 mT; (b) 2.5 K and 6 mT; (c) remnant state of the Co layer at $T = 10$ K.

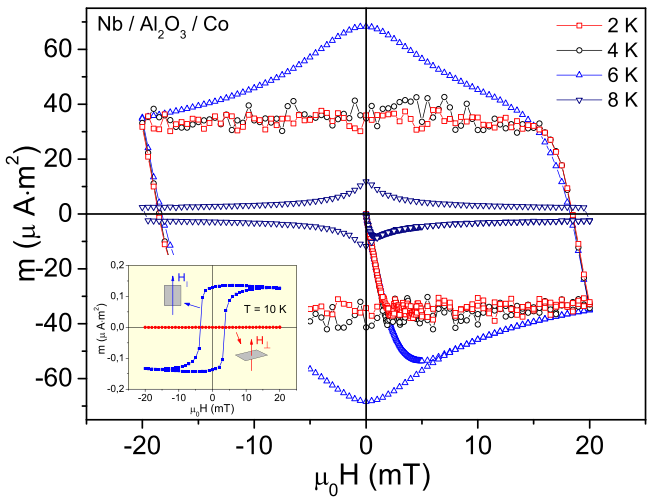

FIG. 2. Magnetic moment versus applied field for the heterostructure $Nb/Al_2O_3/Co$. The noise in the hysteresis loop at $T = 2$ K and $T = 4$ K is typical of the occurrence of flux avalanches.

The magnetic texture produced by flux avalanche remains stable in the Co layer at temperatures well above T_c. As an example, Fig. 4 shows a micrograph of the imprinted flux registered at room temperature. Although some branches merged into a bulky one and others look blurry at this temperature, their observation is an indication of the robustness of the imprinted magnetic structure. At first sight, the textures imprinted in the Co layer as shown in Figs. 3(c) and 4 look as filamentary regions carved into high relief. This appearance is in fact due to a sub-structure formed by a central region where the magnetization remains oriented in-plane, which is bordered by thin and opposite white and dark contours. The magnetization is pointing out, or into, the film in the white, or dark borders, respectively. These thin contours have thicknesses ranging between 10 and 20 μm.

Below room temperature, the application of a magnetic field $H = 1$ T or higher is needed to completely erase the texture imprinted in the Co film.

The flux induced spin texture also affects the field penetration at temperatures where the field penetrates smoothly,

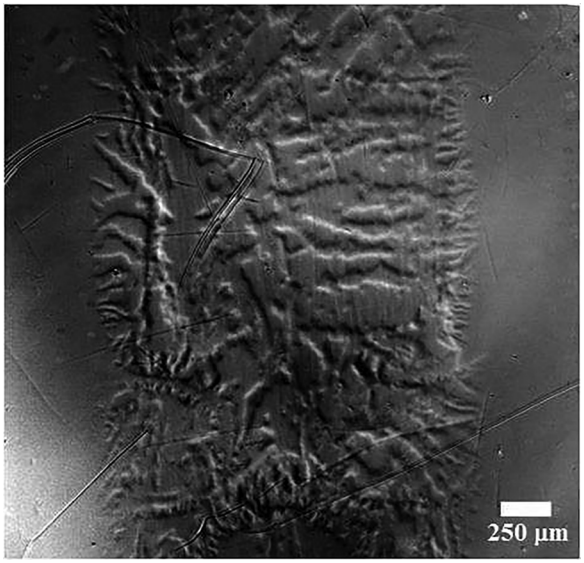

FIG. 4. Magneto-optical imaging of the Co layer showing imprinted vortex avalanches in $T = 300$ K.

as can be observed in Fig. 5. These magneto-optical images were carried out at $T = 8$ K. The difference between the bare Nb and the $Nb/Al_2O_3/Co$ regions is quite visible. In the uncovered Nb film, the flux distribution is homogeneous, while in the $Nb/Al_2O_3/Co$ area magnetic striae appear due to the flux guidance by the previous dendrite imprints. The image (a) was taken at $\mu_0 H = 0.3$ mT. It shows the beginning of flux penetration into the Co area. Increasing the field, as in image (b) taken at $\mu_0 H = 0.6$ mT, the flux occupies the locations magnetized by the avalanches. Clearly, the flux follows the branches and bifurcations left by dendrites. The image (c) was taken at $\mu_0 H = 1$ mT. It shows the surface appearance when the flux is almost fully penetrated into the sample. The flux inhomogeneity takes all over the $Nb/Al_2O_3/Co$ portion that was previously submitted to avalanche occurrences at a lower temperature.

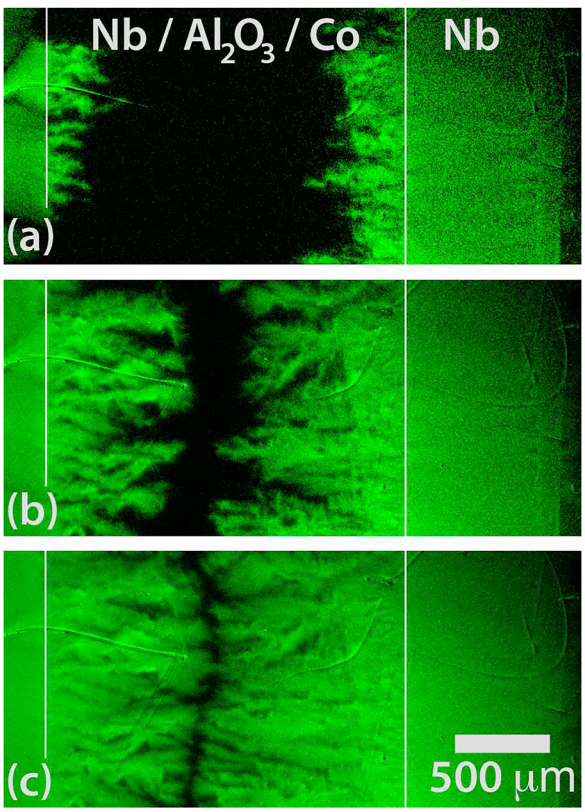

FIG. 5. Magneto-optical imaging at $T = 8$ K (a) $\mu_0 H = 0.3$ mT; (b) $\mu_0 H = 0.6$ mT; (c) $\mu_0 H = 1$ mT.

B. Hall effect and magneto-resistance experiments

In this section, magneto-transport measurements in the $Nb/Al_2O_3/Co$ hybrid are presented and discussed. The results shown are those obtained when the electrical contacts were placed in the ferromagnetic film. We notice that the longitudinal resistivity (results not shown) exhibits a metallic behavior, as usually observed in cobalt thin films.[28] The measured residual resistivity is $\rho_0 \approx 15$ $\mu\Omega$ cm, which is a typical value for a Co film 20 nm thick.[28,29] Moreover, the overall behavior of the magneto-transport data obtained from the Co layer at temperatures above the superconducting T_c of the adjacent Nb film is in good agreement with previously reported results.[28–30]

Figure 6 shows representative Hall resistivity results at low fields in some fixed temperatures below and above T_c. In $T = 2$ K and $T = 4$ K, a rather noisy behavior is observed in ρ_{xy} in the low applied field limit. The noise amplitude is

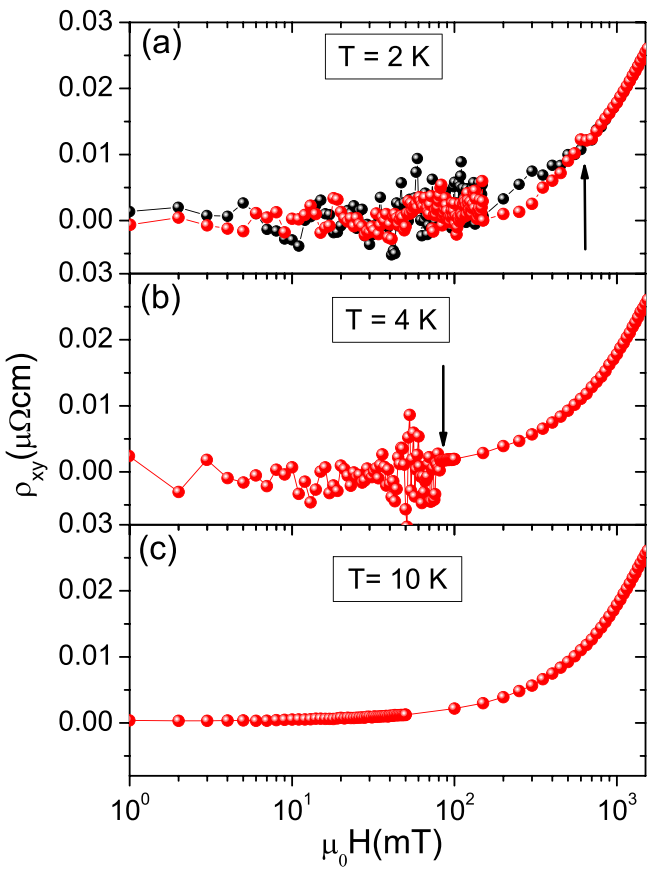

FIG. 6. Low field Hall resistivity as a function of the applied field of the Co layer in the $Nb/Al_2O_3/Co$ hybrid measured in temperatures (a) 2 K, (b) 4 K, and (c) 10 K. Red balls represent results recorded while the field is increased and black symbols correspond to data obtained in decreasing fields. Arrows denote the maximum field for observing instabilities in the ρ_{xy} data.

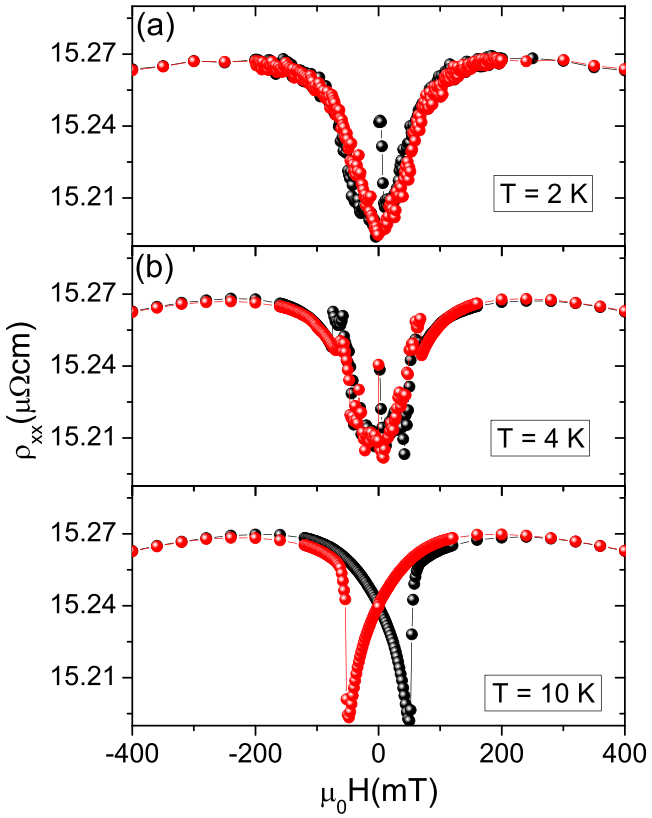

FIG. 7. Low field magneto-resistance of the Co layer in the $Nb/Al_2O_3/Co$ hybrid measured in temperatures (a) 2 K, (b) 4 K, and (c) 10 K. Black balls represent measurements taken as the field increases from $\mu_0 H = -0.4$ T up to $\mu_0 H = +0.4$ T. The data plotted as red balls were obtained while the field was varied in the opposite way.

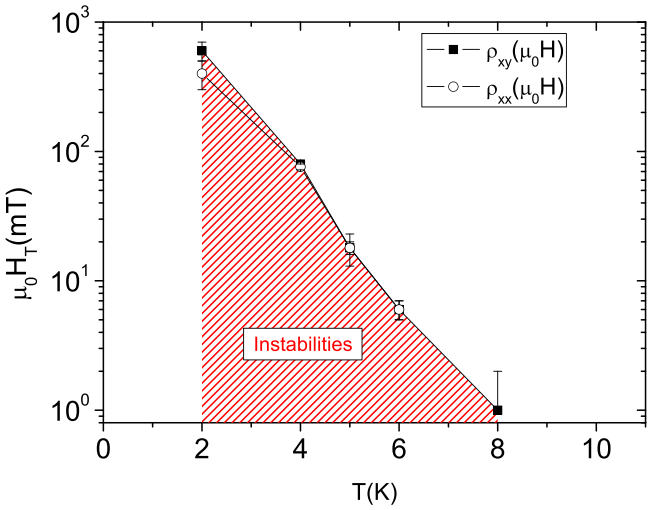

FIG. 8. Characteristic magnetic induction $\mu_0 H_t(T)$ plotted as a function of the temperature for the $Nb/Al_2O_3/Co$ hybrid. The H versus T line drawn through the experimental points denotes the upper limit for observing noisy behavior in the Hall resistivity and magneto-resistance measurements. This line corresponds to the instability boundary for vortex penetration into the Nb layer.

much larger than the experimental resolution of the PPMS. The erratic fluctuations in ρ_{xy} are sharply suppressed above a temperature-dependent threshold field $\mu_0 H_t(T)$, signaled by vertical arrows in Fig. 6. The values obtained for $\mu_0 H_t$ in different isotherms are plotted in the diagram of Fig. 8. These field values define an upper boundary for observing instabilities in the magneto-transport properties. As shown in Fig. 6(c), the noise is not observed in measurements carried out above T_c. We attribute the observed instabilities in $\rho_{xy}(H)$ to successive voltage spikes induced in orientations parallel to the Co layer by the abrupt penetration of the flux dendrites. Indeed, since the average time for avalanche penetration ranges around 0.1 to 0.4 μs,[31,32] the penetration of a single bundle of 100 vortices may produce an easily detectable spike of 1 μV magnitude.

Magneto-resistance (MR) measurements versus the applied field are shown in Fig. 7. The MR shows fluctuations in the same field and temperature intervals as those for the Hall resistivity data. In addition, the usually observed hysteretic behavior in the MR of ferromagnetic metals is rounded off in the temperature range where instabilities were identified in the Co layer of our hybrid. As seen in Fig. 7(c), the normal hysteretic behavior of the MR is restored above T_c.[28] The peaks indicate the position of the coercive field $\mu_0 H_c \cong 0.05$ T. The non-observation of hysteresis in the MR at $T = 2$ K (see Fig. 7(a)) is probably due to a smoothing resulting from rapid inductive fluctuations due to dendritic avalanches. In $T = 4$ K, the MR does not show hysteretic behavior either (Fig. 7(b)). However, the peaks at $\pm H_c$ are discernible though smudged by large amplitude noise.

As for the Hall resistivity, the anomalous fluctuations in ρ_{xx} cease suddenly at the threshold field $\mu_0 H_t(T)$. The values for this characteristic field obtained from the MR measurements are also plotted in Fig. 8.

It is worthwhile to note that a simple device as our trilayer heterostructure allows the detection of flux avalanches using a conventional electrical transport measurement technique. Clearly, in the present stage, the signal detection method employed in our measurements does not allow detailed studies of the noise spectrum as done in the more complex experiments reported in Refs. 31 and 32. However, the use of a normal layer inductively coupled to an electrically isolated superconducting film might be an interesting alternative to study the rapid dynamics of vortex penetration.

In the diagram of Fig. 8, the threshold induction $\mu_0 H_t$ is plotted as a function of the temperature in a logarithmic scale for better visualization of the results in temperatures close to T_c. We propose that this characteristic field defines the upper boundary for the region where vortex instabilities occur in the Nb layer of our heterostructure. Indeed, for field values above $\mu_0 H = 10$ mT and temperatures below $T = 5$ K, the diagram in Fig. 8 reproduces quite nicely similar results reported for Nb films with thicknesses varying from 20 to 500 nm.[22] In the low H–high T region, the diagram in Fig. 8 does not show the reentrance of the instability region in the single layer Nb.[22] Figure 8 suggests instead that $\mu_0 H_t(T)$ approaches zero near T_c. We note that similar enlargements of the H-T region characterized by irregular jumps in magnetization measurements were observed in Nb/permalloy bilayers.[33] Authors in Ref. 33 suggest that the pinning of vortices in channels due to the underlying magnetic domains combined with the intrinsic pinning of the Nb film could

explain the enlargement of the *H-T* domain where vortex instabilities are observed.

IV. FINAL CONSIDERATIONS AND CONCLUSION

Our magneto-optical experiments in $Nb/Al_2O_3/Co$ heterostructures clearly show that dendrites produced by flux avalanches in the Nb layers generate a template consisting of magnetic textures in the adjacent Co layer. The dynamics of the avalanches induces anomalous noise in magneto-transport properties of the Co film. Magnetization measurements in these tri-layer heterostructures show irregular jumps consistently both with MOI experiments and magneto-transport results.

At this stage of the investigation, we should consider the possibility that the spin textures revealed in Fig. 3(c) are related to magnetic domains polarized perpendicularly to the film surface, following the geometry dictated by the flux penetration into the Nb layer. However, it was shown with magnetic force microscopy that in Co films having 20 nm thickness, which is close to that of the Co layer in our hybrid, only domains with in-plane magnetization are stable.[28] Thus, it might be difficult to conceive that thin and extended domains with perpendicular magnetization would subsist in the absence of vortices and applied fields in the Co layer of the studied heterostructure. Moreover, a rough estimation shows that the magnetic energy density transferred by vortices to the ferromagnetic film is not enough to overcome the in-plane shape anisotropy energy for a thin Co film, which is of the order $K = 1.3 \times 10^6\,J/m^3$, as reported in Ref. 34.

Due to the similarities between the vortex lattice in superconductors and the skyrmion lattice in magnetic materials, however, one cannot exclude the possibility that the magnetization texture observed in the Co layer of our $Nb/Al_2O_3/Co$ hybrid is partially formed by skyrmions or some other non-conventional spin chiral-type or vortex-type structures when examined at the microscopic scale. These structures might be searched mainly in the borders of filamentary magnetic textures, where the contrasting dark and white thin contours indicate the occurrence of out-of-plane magnetization.

As a final remark, we mention that the imprinting of vortex avalanches in a ferromagnetic thin film might represent a step forward to the development of an alternative technique for achieving vortex decoration in a medium useful for data recording and processing.

ACKNOWLEDGMENTS

We acknowledge Dr. Eduardo M. Bittar from the Centro Brasileiro de Pesquisas Físicas (CBPF) for invaluable help during the realization of the magneto-transport experiments. One of the authors (RFL) acknowledges the Brazilian agency "Conselho Nacional de Pesquisas Científicas e Tecnológicas" (CNPq) for financial support. The agencies "Fundação de Amparo à Pesquisa do Estado do Rio de Janeiro (FAPERJ)" and "Fundação de Amparo à Pesquisa do Estado de São Paulo" (FAPESP) are also acknowledged.

[1]*Magnetism, Vol. III: Spin Arrangements and Crystal Structure, Domains and Micromagnetism*, edited by G. T. Rado and H. Suhl (Academic Press, London, 1963).
[2]S. A. Wolf, D. D. Awschalom, R. A. Buhrman, J. M. Daughton, S. von Molnár, M. L. Roukes, A. Y. Chtchelkanova, and D. M. Treger, Science **294**, 1488 (2001).
[3]V. Gehanno, A. Marty, B. Gilles, and Y. Samson, Phys. Rev. B **55**, 12552 (1997).
[4]T. Fukumura, H. Sugawara, H. Hasegawa, K. Tanaka, H. Sakaki, T. Kimura, and Y. Tokura, Science **284**, 1969 (1999).
[5]Y. Z. Wu, C. Won, A. Scholl, A. Doran, H. W. Zhao, X. F. Jin, and Z. Q. Qiu, Phys. Rev. Lett. **93**, 117205 (2004).
[6]T. Shinjo, T. Okuno, R. Hassdorf, K. Shigeto, and T. Ono, Science **289**, 930 (2000).
[7]C. Day, Phys. Today **62**(4), 12 (2009).
[8]Y. Machida, S. Nakatsuji, Y. Maeno, T. Tayama, T. Sakakibara, and S. Onoda, Phys. Rev. Lett. **98**, 057203 (2007).
[9]D. Hsieh, Y. Xia, L. Wray, D. Qian, A. Pal, J. H. Dil, J. Osterwalder, F. Meir, G. Bihlmayer, C. L. Kane, Y. S. Hor, R. J. Cava, and M. Z. Hasan, Science **323**, 919 (2009).
[10]S. Mühlbauer, B. Binz, F. Jonietz, C. Pfleiderer, A. Rosch, A. Neubauer, R. Giorgii, and P. Böni, Science **323**, 915 (2009).
[11]A. Neubauer, C. Pfleiderer, B. Binz, A. Rosch, R. Ritz, P. G. Niklowitz, and P. Böni, Phys. Rev. Lett. **102**, 186602 (2009).
[12]X. Z. Yu, Y. Onose, N. Kanazawa, J. H. Park, J. H. Han, Y. Matsui, N. Nagaosa, and Y. Tokura, Nature **465**, 901 (2010).
[13]S. Heinze, K. V. Bergmann, M. Menzel, J. Brede, A. Kubetzka, R. Wiensendanger, G. Bihlmayer, and S. Blügel, Nat. Phys. **7**, 713 (2011).
[14]A. Fert, V. Cros, and J. Sampaio, Nat. Nanotechnol. **8**, 152 (2013); and references therein.
[15]J. Brisbois, M. Motta, J. I. Avila, G. Shaw, T. Devillers, N. M. Dempsey, S. K. P. Veerapandian, P. Colson, B. Vanderheyden, P. Vanderbemden, W. A. Ortiz, N. D. Nguyen, R. B. G. Kramer, and A. V. Silhanek, Sci. Rep. **6**, 27159 (2016).
[16]V. K. Vlasko-Vlasov, F. Colauto, T. Benseman, D. Rosenmann, and W.-K. Kwok, Sci. Rep. **6**, 36847 (2016).
[17]D. Stamopoulos and E. Aristomenopoulou, J. Appl. Phys. **116**, 233908 (2014).
[18]A. I. Buzdin, Rev. Mod. Phys. **77**, 935 (2005).
[19]M. Berciu, T. G. Rappoport, and B. Jankó, Nature **435**, 71 (2005).
[20]J. Fritzshe, R. B. G. Kramer, and V. V. Moshchalkov, Phys. Rev. B **79**, 132501 (2009).
[21]A. A. Abrikosov, *Fundamentals of the Theory of Metals* (North Holland, Amsterdam, 1988).
[22]F. Colauto, E. J. Patiño, M. G. Blamire, and W. A. Ortiz, Supercond. Sci. Technol. **21**, 045018 (2008).
[23]T. H. Johansen, M. Baziljevich, H. Bratsberg, Y. M. Galperin, P. Lindelof, Y. Shen, and P. Vase, Phys. Rev. B **54**, 16264 (1996).
[24]L. Helseth, R. Hansen, E. Ilyashenko, M. Baziljevich, and T. H. Johansen, Phys. Rev. B **64**, 174406 (2001).
[25]F. Colauto, E. M. Choi, J. Y. Lee, S. I. Lee, V. V. Yurchenko, T. H. Johansen, and W. A. Ortiz, Supercond. Sci. Technol. **20**, L48 (2007).
[26]T. H. Johansen, M. Baziljevich, D. V. Shantsev, P. E. Goa, Y. M. Galperin, W. N. Kang, H. J. Kim, E. M. Choi, M.-S. Kim, and S. I. Lee, Supercond. Sci. Technol. **14**, 726 (2001).
[27]J. Albrecht, A. T. Matveev, M. Djupmyr, G. Schütz, B. Stuhlhofer, and H.-U. Habermeier, Appl. Phys. Lett. **87**, 182501 (2005).
[28]W. Gil, D. Görlitz, M. Horisberger, and J. Kötzler, Phys. Rev. B **72**, 134401 (2005).
[29]A. B. Pakhomov, J. C. Denardin, O. F. de Lima, M. Knobel, and F. P. Missell, J. Magn. Magn. Mater. **226–230**, 1631 (2001).
[30]J. Kötzler and W. Gil, Phys. Rev. B **72**, 060412 (2005).
[31]P. Mikheenko, A. J. Quiller, J. I. Vesgarden, S. Chaudhuri, I. J. Maasilta, Y. M. Galperin, and T. H. Johansen, Appl. Phys. Lett. **102**, 022601 (2013).
[32]P. Mikheenko, T. H. Johansen, S. Chaudhuri, I. J. Maasilta, and Y. M. Galperin, Phys. Rev. B **91**, 06507(R) (2015).
[33]M. Lavarone, A. Scarfato, F. Booba, M. Longobardi, S. A. Moore, G. Karapetrov, V. Yefremenko, V. Novosad, and A. M. Cucolo, IEEE Trans. Magn. **48**, 3275 (2012).
[34]F. Cardarelli, *Materials Handbook: A Concise Desktop Reference*, 2nd ed. (Springer, 2008), p. 502.